Electronic Supplementary Information (ESI)

Light-Emitting Conjugated Microporous Polymers Based on Excited-State Intramolecular Proton Transfer Strategy and Selective Switch-off Sensing of Anions

Yuwei Zhang,[ab] Qikun Sun,[c] Zhongping Li [bc*] Ziping Li,[b] Yongfeng Zhi,[b] He Li,[d] Hong Xia,[e] and Xiaoming Liu [b*]

[a] Laboratory of Preparation and Applications of Environmental Friendly Materials (Jilin Normal University), Ministry of Education, Changchun, 130103, China.
[b] College of Chemistry, Jilin University, Changchun, 130012, China.
[c] School of Energy and Chemical Engineering, Ulsan National Institute of Science and Technology (UNIST), Ulsan, 44919, Republic of Korea.
[d] State Key Laboratory of Catalysis, Dalian Institute of Chemical Physics, Chinese Academy of Sciences, Dalian, 110621, P. R. China.
[e] State Key Laboratory on Integrated Optoelectronics, College of Electronic Science and Technology, Jilin University, Changchun, 130012, P. R. China.
Corresponding author. E-mail address: lizhongping2020@unist.ac.kr.; xm_liu@jlu.edu.cn.

Section 1. **Instrumental characterization**

Section 2. **¹³C NMR spectra**

Section 3. **Solid-state electronic absorption spectra**

Section 4. **Elemental analysis**

Section 5. **TGA curves**

Section 6. **PXRD patterns**

Section 7. **Isosteric heat of carbon dioxide adsorption**

Section 8. **Fluorescence spectra**

Section 9. **Dynamic light scattering measurement**

Section 10. **¹H NMR spectra**

Section 11. **Plot of PL quenching efficiency**

Section 12. **Fluorescence spectra**

Section 1. **Instrumental characterization**

The infrared spectra were recorded from 500 to 3500 cm^{-1} on an Avatar FT-IR 360 spectrometer by using KBr pellets. Elemental analyses were measured by an Elementar model vario EL cube analyzer. Field emission scanning electron microscopy was recorded on a SU8020 model HITACHI microscope. Powder X-ray diffraction data were performed on a PANalytical BV Empyrean diffractometer by depositing powder on glass substrate, from 2θ = 4.0° to 35° with 0.02°. Thermogravimetric analysis (TGA) was performed on a TA Q500 thermogravimeter with the heating at a rate of 10 °C min^{-1} from 35°C to 800 °C under nitrogen. Nitrogen sorption isotherms were measured at 77 K with a JW-BK 132F analyzer. The absolute fluorescence quantum yields were measured on Edinburgh FLS920 by using an integrating sphere. Photoluminescence spectra were recorded on a Cary Eclipse Fluorescence Spectrophotometer. Frontier molecular orbital (FMO) plots of model-1 and model-2 at the level of B3LYP/6-31G(d,p). CMPs was dispersed in THF to yield a nearly transparent dispersion which was immediately subjected to fluorescence spectroscopy. After the addition anions, time-dependent fluorescence spectra were recorded.
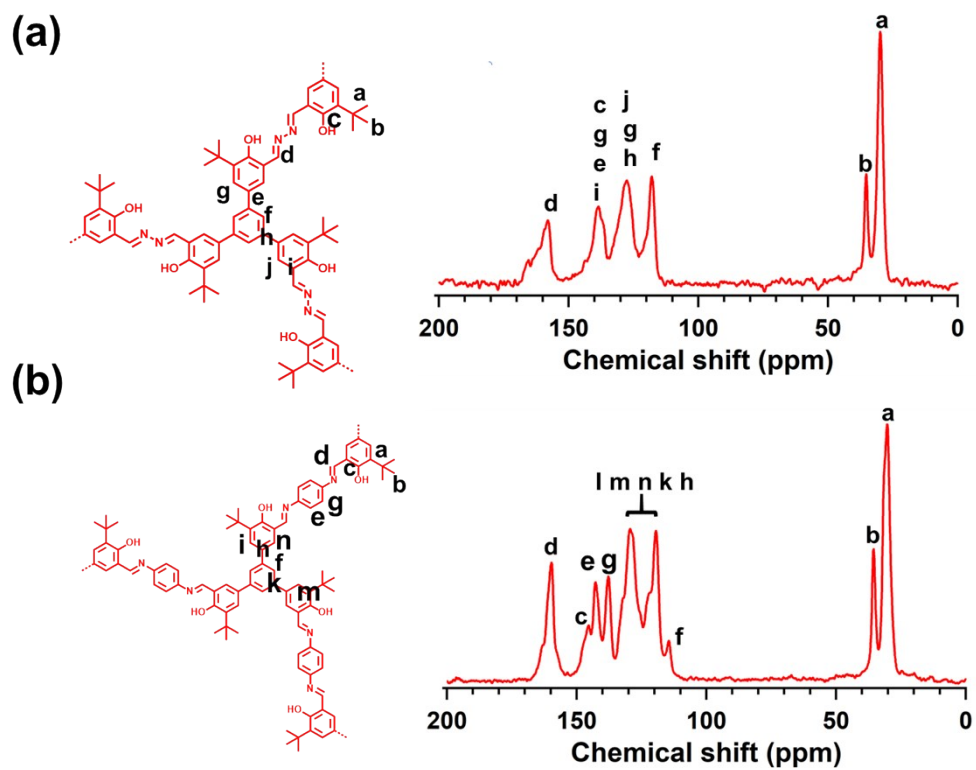
Section 2. ¹³C NMR spectra

(a)

(b)

Fig. S1. ¹³C NMR spectra (a) CMP-A and (b) CMP-B.

2

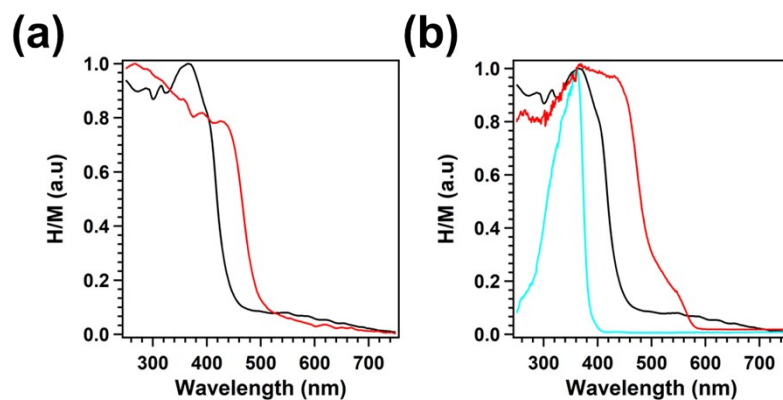**Section 3**. **Solid-state electronic absorption spectra**

Fig. S2. Solid-state electronic absorption spectra of (a) CMP-A (red) and monomer C (black); (b) CMP-B (red), monomer C (black) and monomer B (sky-blue).

Section 4. **elemental analysis**

Table 1

Element Samples		C%	H%	N%
CMP-A	Observed	77.15	7.61	6.91
	Calculated	75.72	6.99	6.68
CMP-B	Observed	80.20	7.01	5.75
	Calculated	80.64.	6.67	5.88

Section 5. **TGA curves**
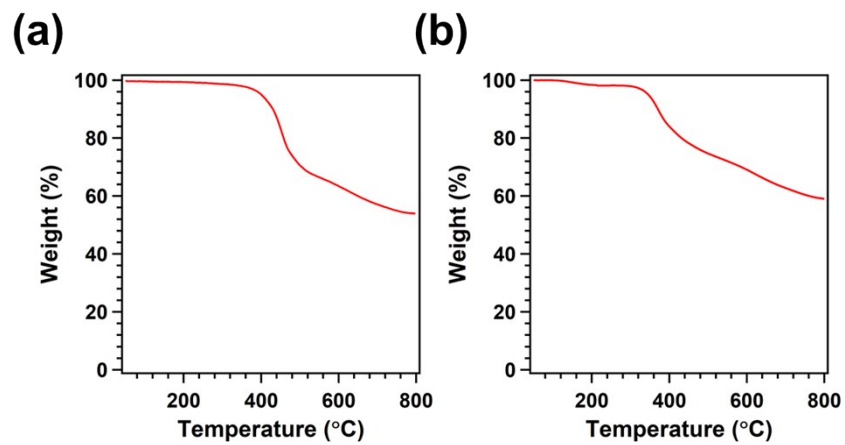
Fig. S3. TGA curves of (a) CMP-A and (a) CMP-B.
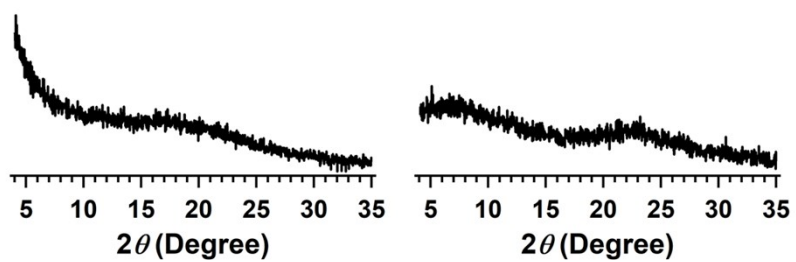
Section 6. **PXRD patterns**

(a)   **(b)**

Fig. S4. PXRD patterns of (a) CMP-A and (a) CMP-B.

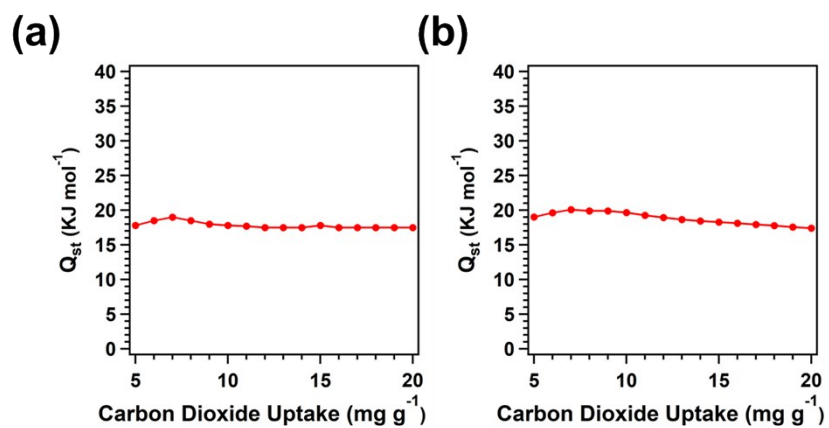**Section 7. Isosteric heat of carbon dioxide adsorption**

Fig. S5. The isosteric heat of adsorption of CO_2 for (a) CMP-A and (b) CMP-B.
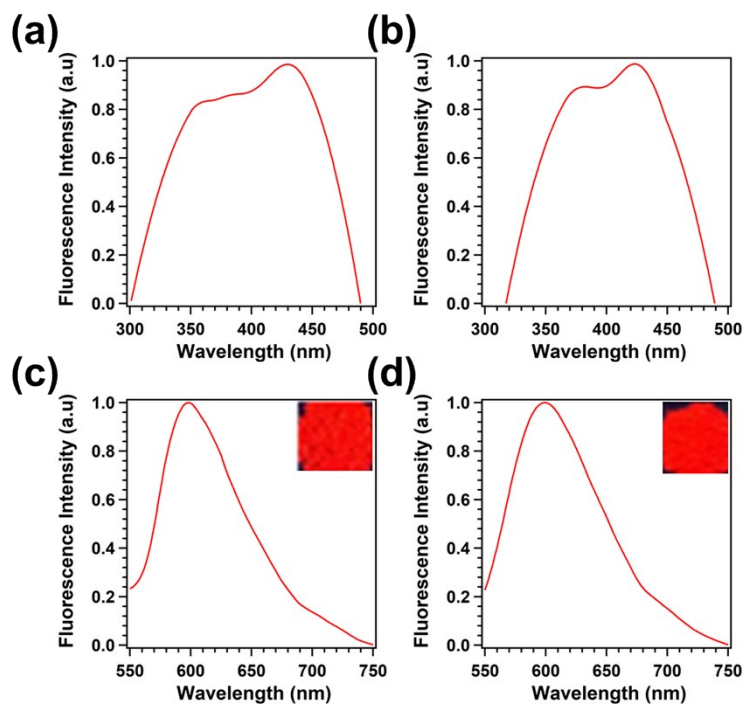
Section 8. **Fluorescence spectra**

Fig. S6. Normalized fluorescence excitation spectra of (a) CMP-A and (b) CMP-B. Normalized fluorescence emission spectra of (c) CMP-A and (d) CMP-B.

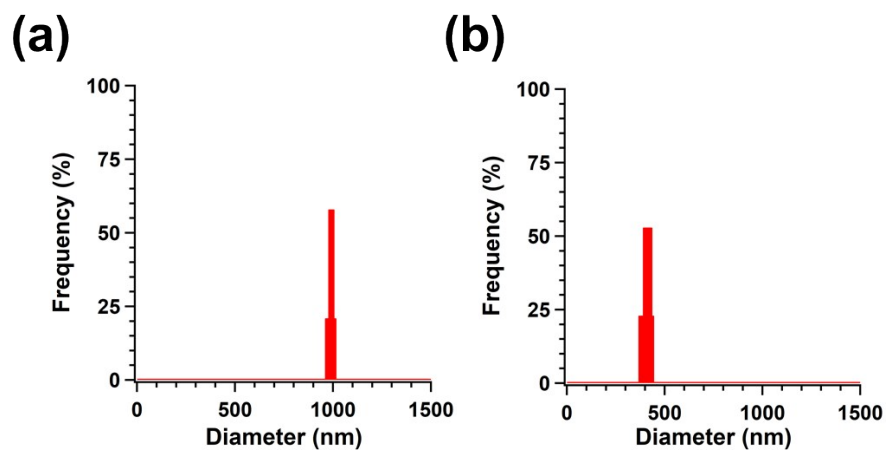**Section 9**. **Dynamic light scattering measurement**

Fig. S7. Dynamic light scattering profile of (a) CMP-A and (b) CMP-B.
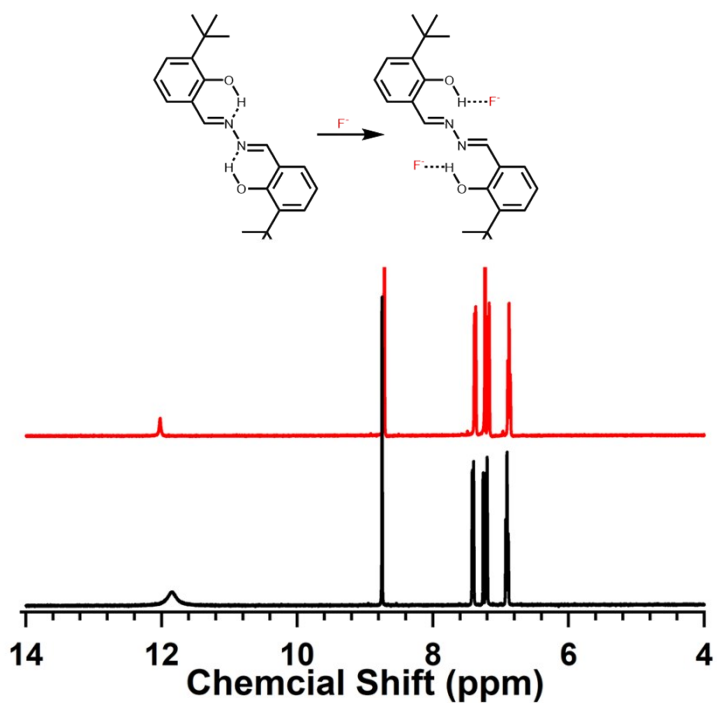
Section 10. ^{1}H NMR spectra

Fig. S8. NMR spectra of module before (black curve) and after fluoride anions (red curve).

Section 11. **Plot of PL quenching efficiency**
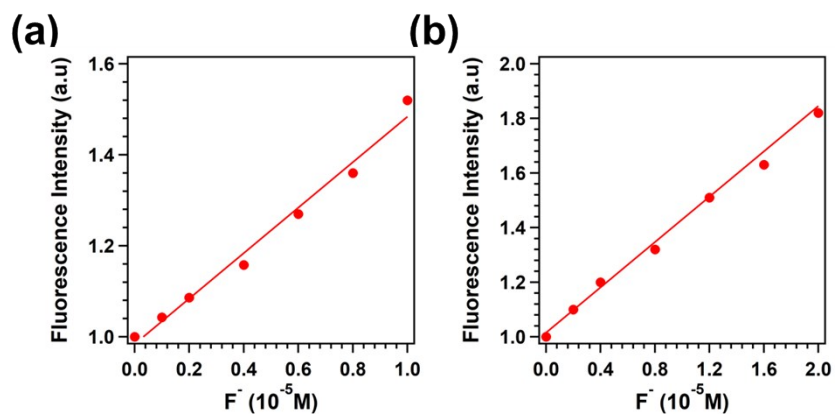
(a)

(b)

Fig. S9. Plot of PL quenching efficiency (I_0/I) as a function of fluoride anions concentration of (a) CMP-A and (b) CMP-B (fluoride anions: 0 to 10^{-4} M).
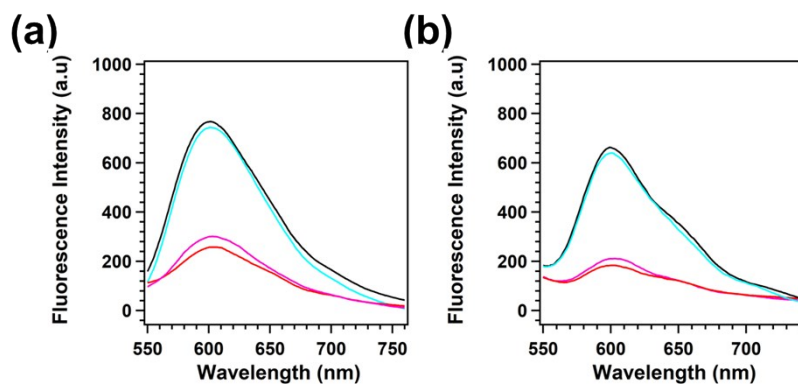
Section 12. **Fluorescence spectra**

Fig. S10. Fluorescence spectra of (a) CMP-A and (b) CMP-B in THF (Original CMPs: black curves; CMPs@F$^-$@H$^+$: sky-blue curves; CMPs@F$^-$@H$^+$@F$^-$: pink curves; CMPs@F$^-$: red curves).